Mutations in the DNA demethylase *OsROS1* result in a thickened aleurone and improved nutritional value in rice grains

Jinxin Liu[a,1], Xiaoba Wu[a,1], Xuefeng Yao[a], Ronald Yu[b], Philip J. Larkin[b], and Chun-Ming Liu[a,c,2]

[a]Key Laboratory of Plant Molecular Physiology, Institute of Botany, Chinese Academy of Sciences, 100093 Beijing, China; [b]Commonwealth Scientific and Industrial Research Organisation, Agriculture and Food, Canberra, ACT 2601, Australia; and [c]Institute of Crop Sciences, Chinese Academy of Agricultural Sciences, 100081 Beijing, China

Edited by Jian-Kang Zhu, Purdue University, West Lafayette, IN, and approved August 21, 2018 (received for review April 12, 2018)

The rice endosperm, consisting of an outer single-cell layer aleurone and an inner starchy endosperm, is an important staple food for humans. While starchy endosperm stores mainly starch, the aleurone is rich in an array of proteins, vitamins, and minerals. To improve the nutritional value of rice, we screened for mutants with thickened aleurones using a half-seed assay and identified *thick aleurone 2–1* (*ta2-1*), in which the aleurone has 4.8 ± 2.2 cell layers on average. Except for starch, the contents of all measured nutritional factors, including lipids, proteins, vitamins, minerals, and dietary fibers, were increased in *ta2-1* grains. Map-based cloning showed that *TA2* encodes the DNA demethylase OsROS1. A point mutation in the 14th intron of *OsROS1* led to alternative splicing that generated an extra transcript, *mOsROS1*, with a 21-nt insertion from the intron. Genetic analyses showed that the *ta2-1* phenotype is inherited with an unusual gametophytic maternal effect, which is caused not by imprinted gene expression but rather by the presence of the *mOsROS1* transcript. Five additional *ta2* alleles with the increased aleurone cell layer and different inheritance patterns were identified by TILLING. Genome-wide bisulfite sequencing revealed general increases in CG and CHG methylations in *ta2-1* endosperms, along with hypermethylation and reduced expression in two putative aleurone differentiation-related transcription factors. This study thus suggests that OsROS1-mediated DNA demethylation restricts the number of aleurone cell layers in rice and provides a way to improve the nutrition of rice.

rice | endosperm | thick aleurone | nutrition | DNA demethylation

The triploid cereal endosperm, consisting of an outer aleurone and an inner starchy endosperm, contributes to >70% of the staple foods consumed by humans (1). Endosperm development commences with coenocytic nuclear division, followed by cytokinesis and differentiation of the aleurone and starchy endosperm (2, 3). Although these two tissues have the same developmental origin, they differ in morphology, cell fate, and storage product accumulation. Starchy endosperm, a dead tissue at maturity, accumulates mainly starch, whereas the aleurone, a living tissue, accumulates mainly storage proteins, lipids, vitamins, and minerals (3, 4).

Most cereal grains have a single-cell layered aleurone; the sole known exception is barley (*Hordeum vulgare*), in which the aleurone has two to three cell layers (5). In rice (*Oryza sativa*), the aleurone is mostly a single cell layer but consists of three or four cell layers in a small, thickened region near the dorsal vascular bundle (3). Several genes involved in aleurone differentiation have been identified in maize (*Zea mays*) and rice. In maize, mutations of *DEFECTIVE KERNEL 1* (*DEK1*) or *CRINKLY4* (*CR4*) lead to partial loss of the aleurone (6, 7). In rice, mutation of a *DEK1* homolog, *ADAXIALIZED LEAF1* (*ADL1*), or suppressed expression of *OsCR4* also causes partial loss of the aleurone cell layer in endosperms (8, 9). In contrast, mutations of *NAKED ENDOSPERM* (*NKD*) transcription factors or a class E vacuolar sorting protein *SUPERNUMERARY ALEURONE LAYER1* (*SAL1*) lead to the formation of endosperms with multiple aleurone cell layers (10, 11). Endosperms with multicell layered aleurone also have been observed in rice when the expression of transcriptional activators *RISBZ1* and *RPBF* are suppressed (12). Since all these grains with multicell layered aleurone exhibit severe defects in grain filling, none has been adopted in crop breeding.

DNA methylation plays an essential role in many biological processes, including growth, development, and stress responses (13). In plants, DNA methylation commonly occurs at the cytosine (C) residue in both the symmetrical CG and CHG and the asymmetrical CHH sequence contexts (H = A, C, or T), and is regulated dynamically by balanced methylation and demethylation (13). Previous studies have identified several enzymes underlying active DNA demethylation in *Arabidopsis*. *DEMETER* (*DME*), expressed in the central cell of the female gametophyte and the early endosperm, is critical for establishing imprinted expression of *MEDEA* by allele-specific demethylation (14, 15). A paralog of *DME*, *ROS1*, is constitutively expressed and regulates gene expression by preventing the spread of DNA methylation and transcriptional silencing from transposons (16, 17). In rice, a knockout mutation of the *ROS1* homolog, *OsROS1*, is defective in both male and female gametogenesis and thus produces no seeds (18).

To improve the nutritional value of rice, we screened for mutants with thickened aleurone using a forward genetic approach and

Significance

The aleurone, storing proteins, lipids, vitamins, and minerals, is the most nutritious part of cereal grains. Genetic analyses were conducted to screen for mutants with thickened aleurone, and identified *thick aleurone 2-1*, which exhibits a multicell-layered aleurone and an improved nutritional profile. Map-based cloning showed that *TA2* encodes a DNA demethylase. This study provides a strategy for enhancing the nutritional value of rice, and possibly of other cereals as well.

Author contributions: C.-M.L. designed research; J.L. and X.W. performed research; X.Y. and R.Y. contributed new reagents/analytic tools; J.L. and C.-M.L. analyzed data; and J.L., P.J.L., and C.-M.L. wrote the paper.

The authors declare no conflict of interest.

This article is a PNAS Direct Submission.

Data deposition: The sequencing data reported in this paper have been deposited in the Gene Expression Omnibus (GEO) database, https://www.ncbi.nlm.nih.gov/geo/ (accession no. GSE117187).

[1]J.L. and X.W. contributed equally to this work.

[2]To whom correspondence should be addressed. Email: cmliu@ibcas.ac.cn.

This article contains supporting information online at www.pnas.org/lookup/suppl/doi:10.1073/pnas.1806304115/-/DCSupplemental.

Published online October 1, 2018.

identified the *thick aleurone 2–1* (*ta2-1*) mutant, which exhibits enhanced contents of a large set of nutritional factors. The *thick aleurone* (*ta*) phenotype is inherited via an unusual gametophytic maternal effect. Molecular genetic analyses revealed that the phenotype is caused by the presence of a malfunctioning *mOsROS1* transcript with a dominant negative effect.

Results

The *ta2-1* Mutant Exhibits an Increased Number of Aleurone Cell Layers. To identify mutants with the *ta* phenotype, we screened approximately 36,000 M3 grains from more than 6,000 ethyl methanesulfonate-mutagenized M2 rice plants (*Oryza sativa*, *Geng* var. Zhonghua 11, ZH11) using a half-seed assay (Fig. 1*A*). Dehusked mature grains without visible defects were selected, sectioned transversally with a razor blade into two halves, and placed on two parallel 96-well plates. The halves without embryos were stained with Evans blue, a dye that stains dead tissues by penetrating membranes with compromised integrity, which allowed us to distinguish the starchy endosperm, which was stained blue, from the aleurone, which was not stained (Fig. 1*B*). This screening, performed under a dissecting microscope, allowed us to identify 24 putative *ta* lines. The corresponding halves with embryos were then sterilized and germinated in vitro on 1/2 MS basal salt medium with 1% sucrose (Fig. 1*A*). Examination of the M4 grains thus produced allowed us to identify the *ta2-1* mutant characterized in detail in this study.

The *ta* phenotype of *ta2-1* was recognizable in both transversally (Fig. 1*B*) and longitudinally (Fig. 1*C*) sectioned grains stained with Evans blue and was confirmed by counterstaining with Sudan red IV, which stains lipids, and Lugol's iodine, which stains starch (*SI Appendix*, Fig. S1 *A* and *B*). Cytohistological analysis performed on semithin sectioned *ta2-1* grains, stained with periodic acid-Schiff (PAS) reagent and Coomassie brilliant blue (CBB), showed that instead of having mostly a single-cell layered aleurone in ZH11, the aleurone of *ta2-1* consisted of 2–12 cell layers, with an average of 4.8 ± 2.2 layers (Fig. 1 *D* and *E* and *SI Appendix*, Fig. S1 *C* and *D*). In contrast to the semitransparent grains of the wild type, some of the *ta2-1* grains were opaque (*SI Appendix*, Fig. S1 *E* and *F*). The differences in aleurones between ZH11 and *ta2-1* endosperms were recognizable at 7 d after pollination (DAP) and were more pronounced from 9 DAP onward (Fig. 1*F* and *SI Appendix*, Fig. S2).

We examined various agronomic traits after five backcrosses and found that most of these traits in *ta2-1* exhibited no detectable defects (*SI Appendix*, Fig. S3 *A–K*). However, the 1,000-grain weight and seed setting rate of *ta2-1* were reduced by 5.9% and 8.2%, respectively (*SI Appendix*, Fig. S3 *L* and *M*), which led to a 12.1% decrease in grain yield per plant and an 18.0% decrease in the yield per plot (*SI Appendix*, Fig. S3 *N* and *O*).

***ta2-1* Grains Showed Improved Nutritional Content.** To examine whether the increased number of aleurone cell layers in *ta2-1* led to enhanced nutritional value, we measured the contents of various nutritional factors in the dehusked mature grains of ZH11 and *ta2-1* plants. As expected, the total protein, lipid, iron, zinc, calcium, dietary fiber, antioxidant, phenolic, and vitamin A, B1, B2, B3, B6, and E contents of *ta2-1* grains were significantly higher compared with wild type (Fig. 2 *A–N*), whereas the total starch and amylose contents were slightly lower (Fig. 2 *O* and *P*).

Genetic Analysis of *ta2-1*. Genetic analysis revealed that 49.4% of grains produced by heterozygous plants carrying the *ta2-1* mutation (*TA2*/*ta2-1* hereinafter) exhibited the *ta* phenotype (Table 1). When ZH11 was pollinated by either *ta2-1* or *TA2-1*/*ta2-1*, all grains produced exhibited the wild-type phenotype, whereas when *ta2-1* was pollinated by ZH11 or *TA2-1*/*ta2-1*, all grains exhibited the *ta* phenotype (Table 1 and *SI Appendix*, Fig. S4). Moreover, when *TA2*/*ta2-1* was pollinated by ZH11 or *ta2-1*, approximately 50% of grains exhibited the *ta* phenotype (Table 1). These results suggest that the inheritance of the *ta2-1* trait has a gametophytic maternal effect.

Molecular Cloning of *TA2*. To identify the *TA2* gene, map-based cloning was performed on the progeny of a cross between *ta2-1*

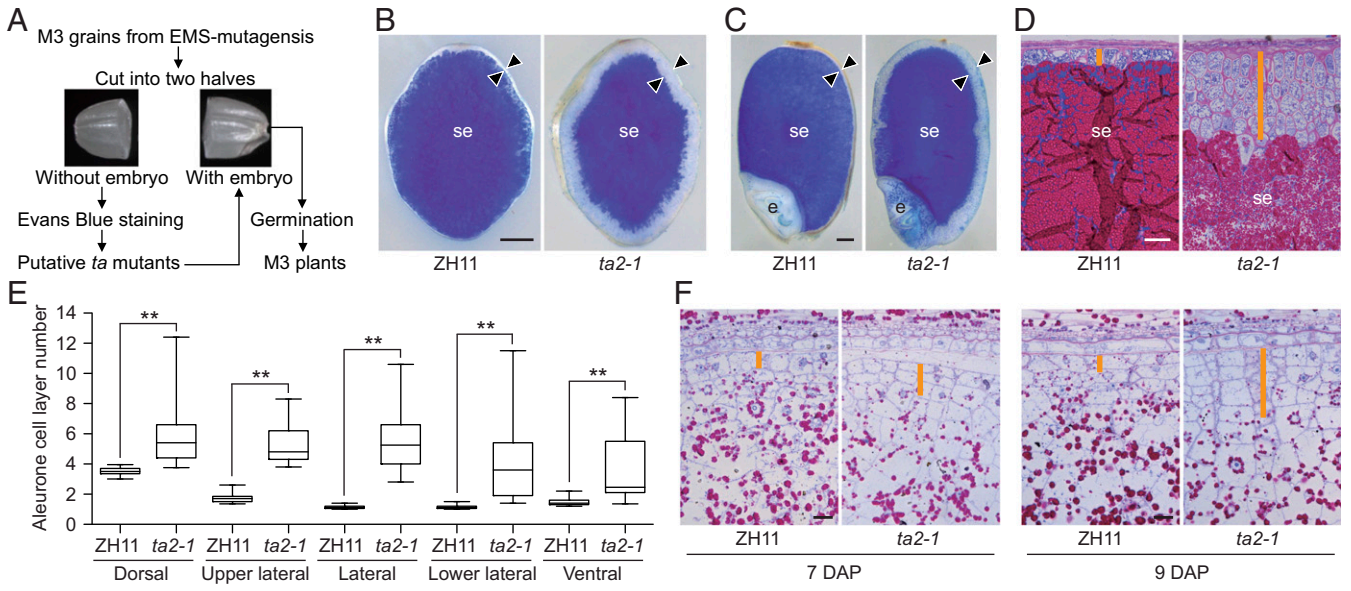

Fig. 1. Identification and characterization of the *ta2-1* mutant. (*A*) Scheme of the genetic screen for *ta* mutants in rice using a half-seed assay. (*B* and *C*) Transversally (*B*) and longitudinally (*C*) sectioned ZH11 and *ta2-1* dehusked mature grains, stained with the cell viability dye Evans blue. (Scale bar: 0.5 mm.) (*D*) Morphology of the aleurone at the lateral positions of ZH11 and *ta2-1* endosperms. (Scale bar: 50 μm.) (*E*) Average numbers of aleurone cell layers, calculated in 20-cell file regions at the dorsal, upper lateral, lateral, lower lateral, and ventral positions of ZH11 and *ta2-1* endosperms ($n = 30$). **Significant differences from ZH11 at the 0.01 level according to Student's *t* test. (*F*) Aleurone at the lateral positions of ZH11 and *ta2-1* endosperms at 7 and 9 DAP. (Scale bar: 20 μm.) Arrowheads in *B* and *C* and orange lines in *D* and *F* indicate the aleurone. e, embryo; se, starchy endosperm.

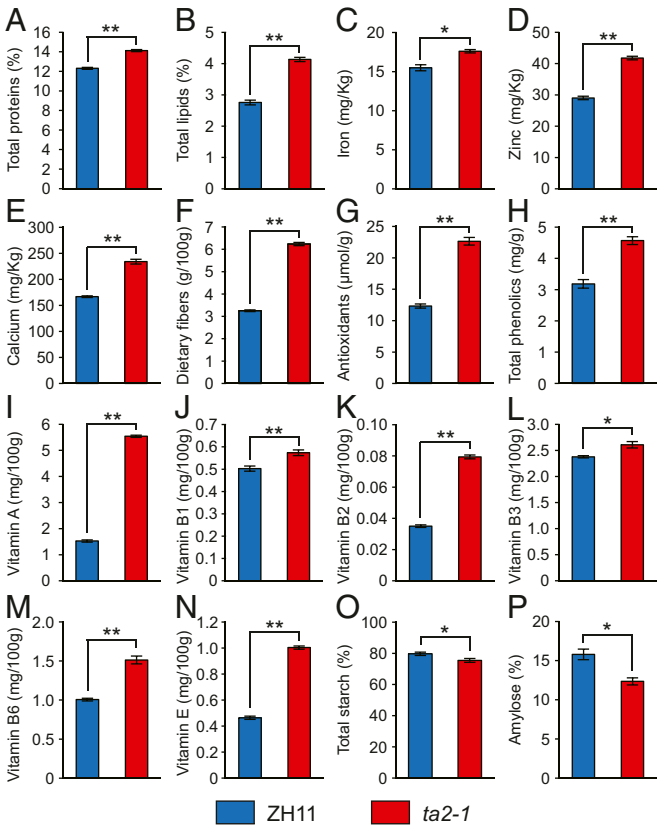

Fig. 2. Improved nutritional content of dehusked mature grains of *ta2-1*. (*A*) Total proteins. (*B*) Total lipids. (*C*) Iron. (*D*) Zinc. (*E*) Calcium. (*F*) Dietary fiber. (*G*) Antioxidants. (*H*) Total phenolics. (*I*) Vitamin A. (*J*) Vitamin B1. (*K*) Vitamin B2. (*L*) Vitamin B3. (*M*) Vitamin B6. (*N*) Vitamin E. (*O*) Total starch. (*P*) Amylose. Data are mean ± SD ($n = 3$). * and ** denote significant differences from ZH11 at the 0.05 and 0.01 levels, respectively, according to Student's *t* test.

and a *Xian* rice variety, Nanjing 6 (NJ6). Using a population of >7,000 F2 individuals, *TA2* was located to a 46-kb genomic region that contains three genes (Fig. 3*A*). Sequence analysis revealed a guanine (G)-to-adenine (A) mutation in the 14th intron of Os01g0218032 in *ta2-1* (Fig. 3*B*). The protein encoded by this gene shared the highest level of sequence identity with ROS1 in *Arabidopsis* (*SI Appendix*, Fig. S5 and Table S1), and thus was designated OsROS1. OsROS1 contains all three conserved domains present in ROS1 and DME in *Arabidopsis* (*SI Appendix*, Figs. S5 and S6).

To examine whether the intronic mutation in *ta2-1* altered the transcription, *OsROS1* cDNA from ZH11 and *ta2-1* endosperms was amplified by reverse transcription PCR (RT-PCR). In addition to the normal *OsROS1* transcript detected in ZH11, another slightly larger one, designated as *mOsROS1,* was found in *ta2-1* (Fig. 3*C*). Sequence analysis revealed the presence of an extra 21 nucleotides originating from the 14th intron of OsROS1 in *mOsROS1*, expected to cause an in-frame insertion of seven amino acid residues (CSNVMRQ) in the conserved C-terminal region of the encoded protein (Fig. 3*D* and *SI Appendix*, Fig. S5).

A 16.1-kb genomic sequence harboring the 4.7-kb 5′ upstream region and the 11.4-kb coding sequence of *OsROS1* was amplified from ZH11 and introduced into *ta2-1* by transformation. Complete complementation of the *ta* phenotype was observed in three independent lines (Fig. 3*E* and *SI Appendix*, Fig. S7), confirming that the *ta2-1* phenotype was a result of a mutation in *OsROS1*.

Furthermore, using an in-house TILLING platform, we identified an additional 23 *ta2* alleles with point mutations in *OsROS1* (*SI Appendix*, Table S2). Among these, five (*ta2-2*–*ta2-6*) exhibited the *ta* phenotype (Fig. 3 *B* and *F* and *SI Appendix*, Fig. S5). The number of aleurone cell layers varied from two to six in *ta2-4*, *ta2-5*, and *ta2-6*, which had mutations in nonconserved regions, and from five to 11 in *ta2-2* and *ta2-3*, which had mutations in the conserved glycosylase domain (*SI Appendix*, Fig. S8).

Genetic analysis in selected alleles showed that the *ta2-3* phenotype was inherited in the same manner as *ta2-1*, while *ta2-4*, *ta2-5*, and *ta2-6* had reduced proportions of grains with the *ta* phenotype (*SI Appendix*, Table S3). Analyses of agronomic traits revealed that while *ta2-3* showed reductions in grain thickness, 1,000-grain weights, seed setting rate, and grain yield per plant, no detectable differences were observed in yield-related traits of *ta2-4*, *ta2-5*, and *ta2-6* (*SI Appendix*, Fig. S9).

Expression of *OsROS1*. Quantitative RT-PCR (qRT-PCR) analysis showed *OsROS1* expression in all tissues examined, with higher expression levels in mature pollen, anthers, and ovaries (Fig. 3*G*). In situ hybridization revealed *OsROS1* expression in the vascular tissue, pollen grain, pericarp, aleurone, and starchy endosperm (*SI Appendix*, Fig. S10). We sequenced the RT-PCR products prepared from endosperms collected at 2, 3, 4, 5, 6, and 8 DAP after reciprocal crosses between ZH11 and NJ6, which had a single nucleotide polymorphism (SNP) in the amplicon of *OsROS1*. Our results showed expression of both maternal and paternal *OsROS1* in all stages examined, with the expected higher maternal expression due to the contribution of two maternal genomes and one paternal genome in the triploid endosperm (Fig. 3*H* and *SI Appendix*, Fig. S11), suggesting that *OsROS1* is not an imprinted gene.

The *mOsROS1* Transcript Caused the *ta* Phenotype in *ta2-1*. The qRT-PCR analysis using primers able to distinguish *OsROS1* from *mOsROS1* showed that the *mOsROS1* transcript was approximately four times more abundant than *OsROS1* in *ta2-1* endosperm (Fig. 4*A*). However, in endosperm produced in ZH11 pollinated by *ta2-1*,

Table 1. Genetic analyses of *ta2-1*

Cross combination	Endosperm phenotype, *n*		Grains with *ta* phenotype, %	*P* for 1:1
	Wild type	*ta*		
TA2/ta2-1 × *TA2/ta2-1*	321	313	49.4	0.7506 (NS)
ZH11 × *ta2-1*	197	0	0	NA
ZH11 × *TA2/ta2-1*	171	0	0	NA
ta2-1 × ZH11	0	589	100	NA
ta2-1 × *TA2/ta2-1*	0	422	100	NA
TA2/ta2-1 × ZH11	199	193	49.2	0.7618 (NS)
TA2/ta2-1 × *ta2-1*	212	214	50.2	0.9228 (NS)

NA, not applicable; NS, not significant.

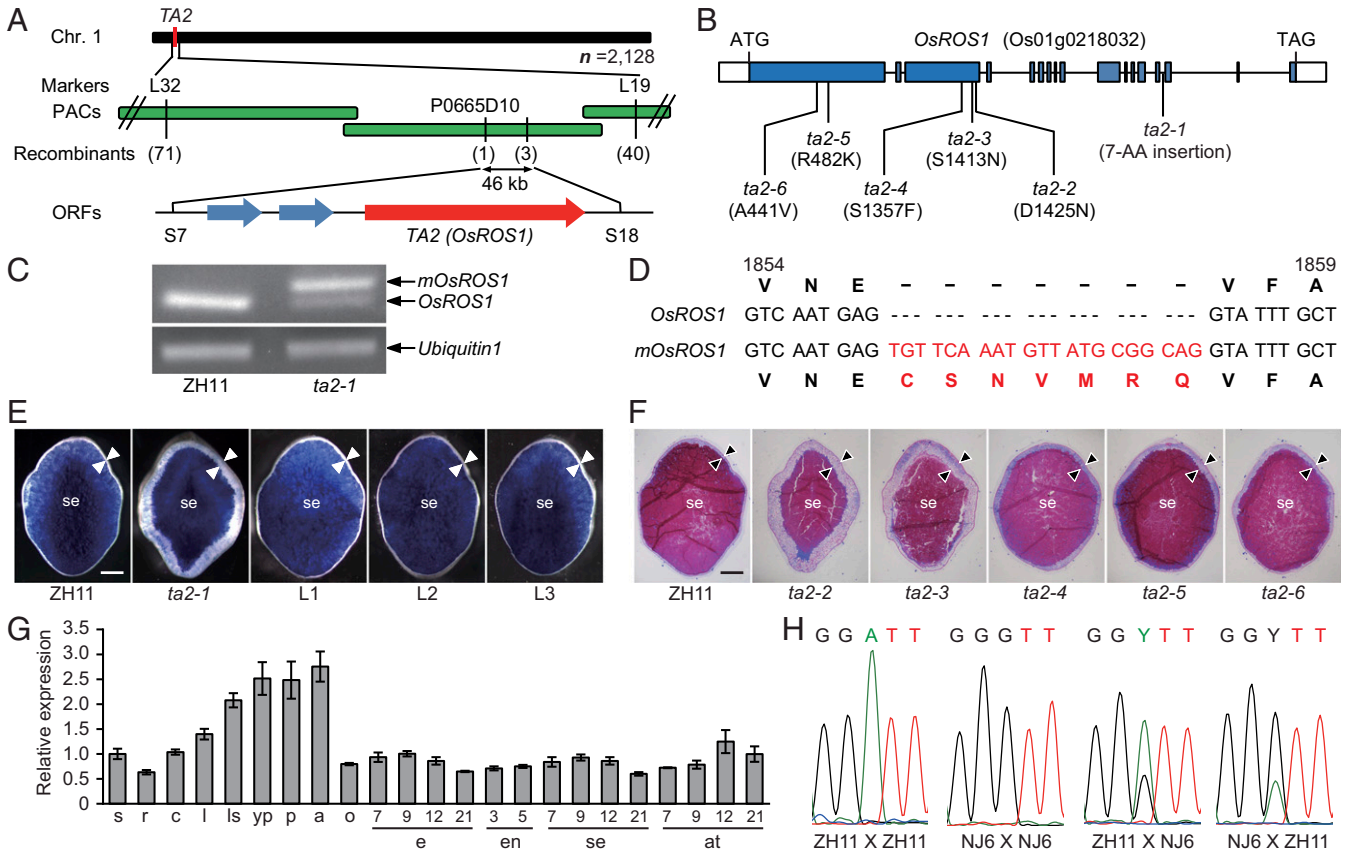

Fig. 3. Molecular characterization of *TA2*. (*A*) *TA2* was mapped to chromosome 1. Numbers of recombinants are indicated in parentheses. (*B*) The *TA2/OsROS1* gene model and mutations in *ta2-1* and TILLING alleles, with mutated amino acids indicated in parentheses. AA, amino acid. (*C*) Two types of transcripts are present in *ta2-1*: a normal *OsROS1* and a slightly larger *mOsROS1*. *Ubiquitin* served as a control. (*D*) *mOsROS1* had a 21-nt insertion from the 14th intron of *OsROS1*, resulting in an in-frame insertion of seven amino acids. (*E*) Transversally sectioned dehusked grains of ZH11, *ta2-1*, and three independent *ta2-1* transgenic lines (L1, L2, and L3) carrying *pCAMBIA1300-OsROS1,* stained with Evans blue, to show complete complementation. (Scale bar: 0.5 mm.) (*F*) Semithin sections of the dehusked mature grains of ZH11 and *ta2-2–ta2-6,* stained with PAS and CBB. (Scale bar: 0.5 mm.) (*G*) Relative expression levels of *OsROS1* in various tissues of ZH11: seedlings (s), roots (r), culms (c), young leaves (l), leaf sheaths (ls), young panicles (yp), mature pollen (p), mature anthers (a), ovaries before anthesis (o), embryos (e), endosperm (en), starchy endosperm (se), and mixed aleurone and testa samples (at) at different DAPs. Values are plotted relative to *OsROS1* expression in seedlings, which was set to 1. Data are mean ± SD ($n = 3$). (*H*) Sequencing chromatographs of RT-PCR products, with an SNP (A or G) in the amplicon, to show the relative abundance of maternal and paternal *OsROS1* transcripts in 2-DAP endosperms after reciprocal crosses between ZH11 and NJ6, with the female parent written first. Y represents the presence of both A and G. Arrowheads in *E* and *F* indicate the aleurone. se, starchy endosperm.

the *mOsROS1* transcript was only roughly one-eighth as abundant as *OsROS1* (Fig. 4*A*). The two transcripts were approximately equally abundant in endosperms produced in *ta2-1* plants pollinated by ZH11 (Fig. 4*A*). We thus propose that the *ta* phenotype is positively associated with the dosage of the *mOsROS1* transcript, such that when ≥50% of the transcripts produced are *mOsROS1*, the *ta* phenotype is inevitable.

To validate this hypothesis, we generated transgenic ZH11 plants carrying either *pUbi*::*OsROS1* (*OE*) or *pUbi*::*mOsROS1* (*mOE*), in which *OsROS1* or *mOsROS1*, respectively, was overexpressed under control of the maize *Ubiquitin 1* promoter (*pUbi*). While none of the *OE* lines exhibited the *ta* phenotype, three independent *mOE* lines showed the *ta* phenotype (Fig. 4 *C* and *D*). In *mOE* plants, the thickness of the aleurone was positively associated with the expression level of the *mOsROS1* transcript (Fig. 4 *B–D*). These observations confirm that the gametophytic maternal effect observed in *ta2-1* is caused by the dominant negative effect of *mOsROS1*.

The Role of OsROS1 in CG and CHG Demethylation in Endosperms. To investigate the function of OsROS1 in DNA demethylation in rice endosperm, we performed whole-genome bisulfite sequencing (WGBS) using DNA extracted from embryos and endosperms of ZH11 and *ta2-1* grains, and then analyzed the distribution of DNA methylation along the gene bodies, transposable elements (TEs), and their flanking regions. In agreement with previously reported results (19, 20), in ZH11, higher CG, CHG, and CHH methylation levels were observed in the embryo than in the endosperm (Fig. 5 *A* and *B*). Evident higher levels of CG and CHG, but not of CHH, methylation were observed in the *ta2-1* endosperm (Fig. 5 *A* and *B*), suggesting that OsROS1 is involved in CG and CHG demethylation in the endosperm.

We then analyzed differentially methylated regions (DMRs) in the *ta2-1* endosperm collected at 9 DAP. A total of 18,399 DMRs were identified in *ta2-1*, which contained 15,147 hypermethylated DMRs (hyper-DMRs) with an average length of 257 bp (Dataset S1). The average methylation levels of CG and CHG hyper-DMRs in *ta2-1* endosperms were significantly higher than those in ZH11 (*SI Appendix*, Fig. S12*A*), which is consistent with the role of OsROS1 in DNA demethylation. Among these hyper-DMRs, 43.2% ($n = 6,548$) were located in TE regions, 38.7% ($n = 5,860$) were located in intergenic regions, 13.5% ($n = 2,042$) were located in genic regions, and 4.6% ($n = 697$) were located in the TE and gene overlapping regions (*SI Appendix*, Fig. S12*B*), indicating that OsROS1, like DME and ROS1 in *Arabidopsis*, preferentially targets TEs and intergenic regions.

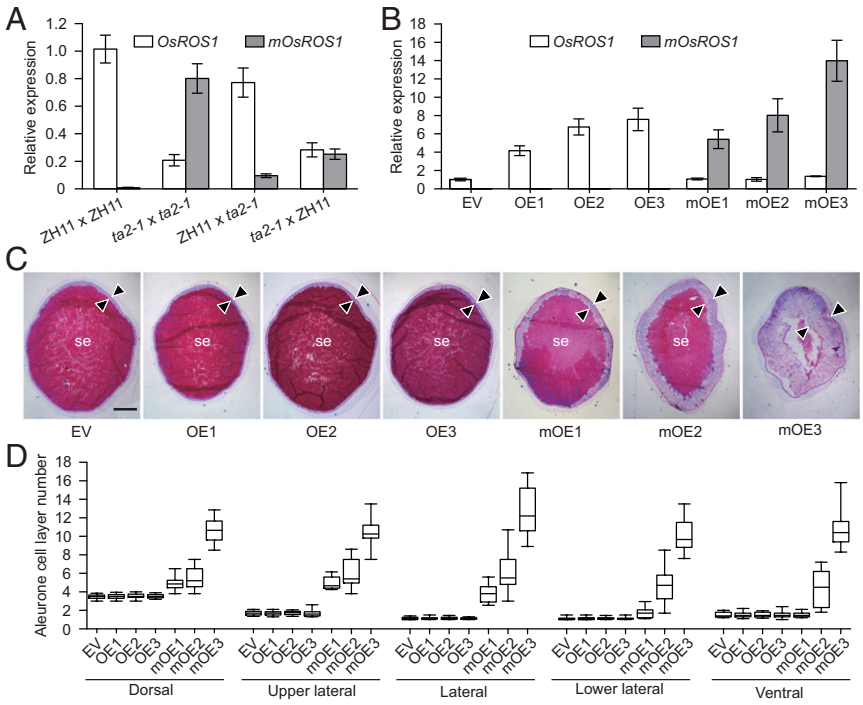

Fig. 4. The presence of *mOsROS1* led to the *ta* phenotype. (*A*) qRT-PCR showing the relative abundance of *OsROS1* and *mOsROS1* transcripts in 9-DAP endosperms produced in crosses between ZH11 and *ta2-1*, with the female parent written first. Values are plotted relative to the expression of *OsROS1* in endosperms of ZH11 × ZH11, which was set to 1. Data are shown as mean ± SD (n = 3). (*B*) Relative *OsROS1* and *mOsROS1* transcript levels in 9-DAP endosperms in transgenic plants carrying an empty vector (EV), *pUbi*::*OsROS1* (lines OE1–OE3), or *pUbi*::*mOsROS1* (lines mOE1–mOE3). Values are plotted relative to the expression of *OsROS1* in transgenic lines carrying an EV, which was set to 1. Data are shown as mean ± SD (n = 3). (*C*) Endosperm phenotypes of EV, OE, and mOE plants. Arrowheads indicate the aleurone. se, starchy endosperm. (Scale bar: 0.5 mm.) (*D*) Average numbers of aleurone cell layers, calculated in 20-cell file regions at different positions of endosperms in EV, OE, and mOE plants (n = 15).

Hypermethylation and Reduced Expression of *RISBZ1* and *RPBF* in *ta2-1*. To identify the potential targets responsible for the *ta* phenotype, the DNA methylation and expression levels of genes known to be involved in aleurone differentiation were analyzed in endosperms at 9 DAP. In *ta2-1* endosperms, the expression levels of *OsNKD1* and *OsDEK1* were not affected (*SI Appendix*, Fig. S13 *A* and *B*), whereas the expression levels of *RISBZ1* and *RPBF* were significantly reduced (Fig. 5 *C* and *D*). By scanning the DNA methylation

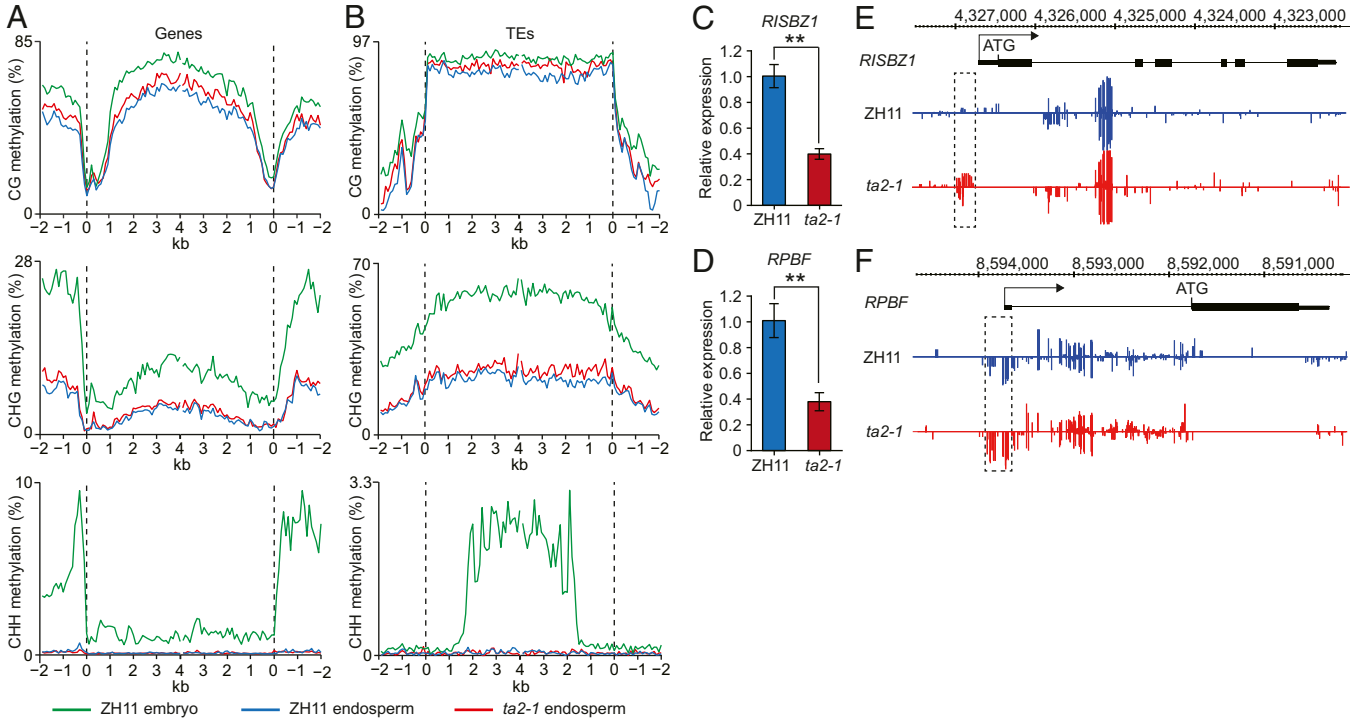

Fig. 5. Altered DNA methylation and gene expression in *ta2-1* endosperms revealed by WGBS. (*A* and *B*) Distribution of DNA methylation levels along gene bodies (*A*) and TEs (*B*) in embryos and endosperms of ZH11 and *ta2-1* at 9 DAP. (*C* and *D*) Reduced expression levels of *RISBZ1* (*C*) and *RPBF* (*D*) in *ta2-1* 9-DAP endosperms revealed by qRT-PCR. Data are shown as mean ± SD (n = 3). **Significant differences from ZH11 at the 0.01 level according to Student's t test. (*E* and *F*) Snapshots in the Integrated Genome Browser showing DNA methylation levels in the *RISBZ1* (*E*) and *RPBF* (*F*) of ZH11 and *ta2-1* endosperms at 9 DAP. Dashed frames indicate the hypermethylated regions in *ta2-1*.

status of the *RISBZ1* and *RPBF* promoters, we found that a 205-bp region at −68 to −273 bp of *RISBZ1* (Fig. 5*E*) and a 219-bp region at 45 to −174 bp of *RPBF* (Fig. 5*F*) relative to the transcription start site were hypermethylated in the *ta2-1* endosperms. As expected, no obvious difference in *OsNKD1* and *OsDEK1* was observed (*SI Appendix*, Fig. S13 *C* and *D*). These results suggest that DNA hypermethylation in the promoter regions of *RISBZ1* and *RPBF* may compromise the expression of these genes.

Discussion

Nutritional improvement in food crops is an important goal in modern agriculture (21) that is achievable for individual nutritional factors by introducing a single gene, such as ferritin (22), or multiple genes, such as those in folic acid (23) and β-carotenoid biosynthesis (24). The results obtained in this study demonstrate the feasibility of improving the general nutritional profile of rice by screening for *ta* mutants. We showed that weak allele mutations of *OsROS1* led to increased numbers of aleurone cell layers and improved the contents of a large set of nutritional factors.

Four putative 5-methylcytosine DNA demethylase genes (*DME*, *ROS1*, *DML2*, and *DML3*) are present in *Arabidopsis*, and six such genes (*OsROS1*, *OsROS1b*, *OsROS1c*, *OsROS1d*, *OsDML3a*, and *OsDML3b*) are present in rice. *DME* is preferentially expressed in the central cell of the female gametophyte and in early endosperms and activates the expression of *MEDEA* by allele-specific DNA demethylation (14, 15). Thus, mutations of *DME* lead to a seed abortion phenotype with a gametophytic maternal effect (14). In contrast, *ROS1* in *Arabidopsis* is expressed in all tissues examined and is crucial for preventing transcriptional gene silencing by DNA demethylation (16, 17). In this study, we showed that *ta2-1* carries a point mutation in the intronic region of *OsROS1*, leading to the production of an alternatively spliced *mOsROS1* transcript. Expression analysis performed in reciprocal crosses between ZH11 and NJ6 showed that *OsROS1* is not an imprinted gene. Together with the fact that three TILLING alleles (*ta2-4*, *ta2-5*, and *ta2-6*) of *OsROS1* did not show gametophytic maternal effects, our findings suggest that OsROS1 is a functional analog of ROS1, not of DME.

A previous study showed that an *OsROS1* knockout mutant exhibits severe defects in both male and female gametogenesis, and thus is not able to set seed (18). However, we have shown that *ta2-1*, a weak mutant allele of *OsROS1*, exhibits an increased number of aleurone cell layers and an improved nutritional profile. TILLING alleles of *ta2-4*, *ta2-5*, and *ta2-6*, with single amino acid substitutions in the nonconserved domain of OsROS1, do not have defects in yield-related traits. These findings suggest the critical importance of exploring the function and phenotype of a gene with multiple alleles.

Expression and phenotypic analyses of endosperms produced after the reciprocal crosses between ZH11 and *ta2-1,* and by transgenic overexpression of *mOsROS1* in the wild type, indicated that the unusual inheritance pattern of *ta2-1* is caused by the presence of the *mOsROS1* transcript. We noted that the abundance of *mOsROS1* in the endosperm produced in ZH11 plants pollinated by *ta2-1* was lower than expected. Whether this is caused by differential splicing or by suppressed expression of *mOsROS1* remains to be determined.

WGBS analysis revealed increased levels of CG and CHG methylations in the *ta2-1* endosperms, approaching the levels seen in ZH11 embryos, suggesting that OsROS1 functions in CG and CHG demethylation. On examination of methylation levels of putative genes involved in aleurone differentiation (8, 10, 12), we observed that in *ta2-1* endosperms, the promoter regions of two transcription factors, *RISBZ1* and *RPBF*, were hypermethylated, and that the expression levels of these genes were substantially reduced, indicating that they are potential target genes causing the *ta* phenotype.

In summary, our results suggest that active DNA demethylation in rice endosperms, executed by OsROS1, restricts the number of aleurone cell layers. These results highlight the potential for manipulating OsROS1 activity to improve the nutritional value of rice and may have applications in other cereal crops as well.

Materials and Methods

Details on plant growth conditions, histological analyses, nutritional content measurements, agronomic trait analyses, map-based cloning, expression analyses, plant transformations, in situ hybridization, and WGBS are provided in *SI Appendix, Materials and Methods*.

ACKNOWLEDGMENTS. We thank the Chinese Cereal Quality Supervision and Monitoring Center, Ministry of Agriculture and Dr. Tony Bird at CSIRO Health and Biosecurity for their assistance with nutritional analyses. This work was supported by the Ministry of Science and Technology of China (Grant 2016YFD0100501/2014CB943401), the Chinese Academy of Sciences (CAS) Innovation Project "Molecular Modules for Breeding Design" (Grant XDA08010301), and the CAS-Commonwealth Scientific and Industrial Research Organization Bilateral Collaboration Project (GJHZ1406).

1. Food and Agriculture Organization Human Nutrition in the Developing World. Available at www.fao.org/docrep/W0073e/w0073e06.htm. Accessed July 10, 2018.
2. Olsen OA (2004) Nuclear endosperm development in cereals and *Arabidopsis thaliana*. *Plant Cell* 16(Suppl):S214–S227.
3. Wu X, Liu J, Li D, Liu CM (2016) Rice caryopsis development II: Dynamic changes in the endosperm. *J Integr Plant Biol* 58:786–798.
4. Becraft PW, Yi G (2011) Regulation of aleurone development in cereal grains. *J Exp Bot* 62:1669–1675.
5. Jestin L, et al. (2008) Inheritance of the number and thickness of cell layers in barley aleurone tissue (*Hordeum vulgare* L.): An approach using F2-F3 progeny. *Theor Appl Genet* 116:991–1002.
6. Lid SE, et al. (2002) The *defective kernel 1* (*dek1*) gene required for aleurone cell development in the endosperm of maize grains encodes a membrane protein of the calpain gene superfamily. *Proc Natl Acad Sci USA* 99:5460–5465.
7. Becraft PW, Stinard PS, McCarty DR (1996) CRINKLY4: A TNFR-like receptor kinase involved in maize epidermal differentiation. *Science* 273:1406–1409.
8. Hibara K, et al. (2009) The *ADAXIALIZED LEAF1* gene functions in leaf and embryonic pattern formation in rice. *Dev Biol* 334:345–354.
9. Pu CX, et al. (2012) Crinkly4 receptor-like kinase is required to maintain the interlocking of the palea and lemma, and fertility in rice, by promoting epidermal cell differentiation. *Plant J* 70:940–953.
10. Yi G, Neelakandan AK, Gontarek BC, Vollbrecht E, Becraft PW (2015) The *naked endosperm* genes encode duplicate INDETERMINATE domain transcription factors required for maize endosperm cell patterning and differentiation. *Plant Physiol* 167:443–456.
11. Shen B, et al. (2003) *sal1* determines the number of aleurone cell layers in maize endosperm and encodes a class E vacuolar sorting protein. *Proc Natl Acad Sci USA* 100: 6552–6557.
12. Kawakatsu T, Yamamoto MP, Touno SM, Yasuda H, Takaiwa F (2009) Compensation and interaction between RISBZ1 and RPBF during grain filling in rice. *Plant J* 59: 908–920.
13. Zhang H, Lang Z, Zhu JK (2018) Dynamics and function of DNA methylation in plants. *Nat Rev Mol Cell Biol* 19:489–506.
14. Choi Y, et al. (2002) DEMETER, a DNA glycosylase domain protein, is required for endosperm gene imprinting and seed viability in *Arabidopsis*. *Cell* 110:33–42.
15. Gehring M, et al. (2006) DEMETER DNA glycosylase establishes MEDEA polycomb gene self-imprinting by allele-specific demethylation. *Cell* 124:495–506.
16. Gong Z, et al. (2002) *ROS1*, a repressor of transcriptional gene silencing in *Arabidopsis*, encodes a DNA glycosylase/lyase. *Cell* 111:803–814.
17. Tang K, Lang Z, Zhang H, Zhu JK (2016) The DNA demethylase ROS1 targets genomic regions with distinct chromatin modifications. *Nat Plants* 2:16169.
18. Ono A, et al. (2012) A null mutation of *ROS1a* for DNA demethylation in rice is not transmittable to progeny. *Plant J* 71:564–574.
19. Zemach A, et al. (2010) Local DNA hypomethylation activates genes in rice endosperm. *Proc Natl Acad Sci USA* 107:18729–18734.
20. Hsieh TF, et al. (2009) Genome-wide demethylation of *Arabidopsis* endosperm. *Science* 324:1451–1454.
21. Pfeiffer WH, McClafferty B (2007) HarvestPlus: Breeding crops for better nutrition. *Crop Sci* 47(Suppl_3):S88–S105.
22. Goto F, Yoshihara T, Shigemoto N, Toki S, Takaiwa F (1999) Iron fortification of rice seed by the soybean ferritin gene. *Nat Biotechnol* 17:282–286.
23. Storozhenko S, et al. (2007) Folate fortification of rice by metabolic engineering. *Nat Biotechnol* 25:1277–1279.
24. Paine JA, et al. (2005) Improving the nutritional value of golden rice through increased pro-vitamin A content. *Nat Biotechnol* 23:482–487.